Solar Energy Materials & Solar Cells 104 (2012) 92–96

Contents lists available at SciVerse ScienceDirect

Solar Energy Materials & Solar Cells

journal homepage: www.elsevier.com/locate/solmat

Enhancement of power conversion efficiency in GaAs solar cells with dual-layer quantum dots using flexible PDMS film

Hsin-Chu Chen [a], Chien-Chung Lin [b,*], Hau-Vei Han [a], Kuo-Ju Chen [a], Yu-Lin Tsai [a], Yi-An Chang [c], Min-Hsiung Shih [a,d], Hao-Chung Kuo [a], Peichen Yu [a]

[a] Department of Photonics and Institute of Electro-Optical Engineering, National Chiao Tung University, Hsinchu 30010, Taiwan
[b] Institute of Photonic System, National Chiao Tung University, Tainan 711, Taiwan
[c] Department of Physics, National Changhua University of Education, Changhua 500, Taiwan
[d] Research Center for Applied Sciences, Academia Sinica 128 Academia Rd., Sec. 2 Nankang, Taipei 115, Taiwan

ARTICLE INFO

Article history:
Received 7 February 2012
Received in revised form
30 April 2012
Accepted 1 May 2012
Available online 31 May 2012

Keywords:
GaAs solar cell
Quantum dots
Dual-layer
PDMS

ABSTRACT

This study demonstrates the high performance of GaAs solar cells with dual-layer CdS quantum dots (QDs) carried by flexible polydimethylsiloxane (PDMS) film. Several parameters were enhanced, including the short circuit current, fill factor, and power conversion efficiency, which were measured under white light illumination similar to the solar spectrum. The flexible PDMS film was fabricated using the spin-coating technique, and was then used to embed dual-layer CdS QDs. Different concentrations of QDs were applied in this design to test the optimal combination. The proposed scheme enhances power conversion efficiency by 22%, compared to a GaAs solar cell without CdS QDs. The photon down-conversion capability in the ultraviolet (UV) range and additional anti-reflection capability in the longer visible-IR range were verified through the external quantum efficiency.

1. Introduction

Highly efficient solar cells have attracted significant attention because of the recent energy crisis and concerns on green-house gas emissions. Among the various solar cell technologies, GaAs-based solar cells have become important because of their constantly increasing power conversion efficiency (PCE). In the past, researchers have reported multi-junction tandem GaAs-based solar cells with a PCE of up to 40% under an illumination of 240 suns [1]. For a single-junction GaAs device, the best result to date is a PCE of 28% [2], which is still below the Shockley–Queisser limit [3] of 33%. Better usage of the solar spectrum may be necessary to approach this limit. Two aspects must be addressed: 1) allow photons enter the solar cell easily, and 2) acquire the formerly unused part of the solar spectrum. When incident light impinges on the interface of a GaAs solar cell, it creates high Fresnel reflectivity because of the high contrast of the refractive indices between air and the GaAs solar cell. The reflection loss of light can reduce the amount of absorption, and thus, the power conversion efficiency of the solar cell. Researchers have developed different anti-reflection methods to solve this problem, such as a single layer of effective anti-reflective coating (ARC) [4–6], multiple-layer ARCs [7,8], surface texturing [9,10], and nanowire or nanotip structures [11–15]. Among these methods, nanowire or nanotip structures can effectively eliminate this type of reflection and improve cell efficiency omni-directionally. The underlying principle of this design is to introduce an intermediate refractive index layer between the air and the substrate material. This layer can subsequently reduce the Fresnel reflection. However, problems remain for this method, such as the substantial recombination of electron–hole pairs on the nanosized pattern surface, and the possible frailty of the nanostructures. Unlike the complexity of nanostructures, the method of using single or multiple layers of anti-reflective coating (ARC) is at the other end of the spectrum: larger scale, and substantially simpler fabrication. Whereas single or multiple layers of ARC are commercially widespread, they are not highly useful in the ultraviolet (UV) and near-UV range. The high-energy photons in this range can be absorbed in a short distance into the solar cell, but the generated carriers are consumed by the surface traps so quickly that no electrical currents can be drawn. Even with a super-clean surface with no traps or defects, the generated carriers still face the daunting challenge of bulk recombination before they can be collected.

In addition to GaAs-based solar cells, some researchers have explored the II–VI semiconductor nanoparticles or quantum dots (QDs) as an alternative source of photovoltaic power. The advantages of QD materials include their process-engineered bandgap, highly efficient absorption and light-emitting

* Corresponding author.
E-mail address: chienchunglin@faculty.nctu.edu.tw (C.-C. Lin).

0927-0248/$ - see front matter © 2012 Elsevier B.V. All rights reserved.
http://dx.doi.org/10.1016/j.solmat.2012.05.003

properties, low cost, and large area deployment. In the past, QDs have been applied in devices such as light-emitting diodes [16–18], photo-detectors [19,20], and solar cells [21–23]. However, scientists find it difficult to have these QD devices achieve a PCE exceeding 10%. Applying more QD materials on a surface may cause the self-assembly phenomenon and further decrease quantum efficiency. Another common problem in QD devices is the reliability or the lifetime issue: these nanoscale particles do not continue to function well when exposed to air.

Based on the advantages and disadvantages of GaAs- and QD-based devices, the right combination of these two completely different technologies should generate a new class of photovoltaic devices. This study presents a discussion on this possibility using multiple layers of flexible PDMS with QDs sandwiched in between, and laying these PDMS layers on top of GaAs-based solar cells. Chen et al. demonstrated a single layer of QD applied to a silicon solar cell [24], and efficiency improvement in the UV range was limited by the amount of down-converted photons that a single layer of QDs can generate. When QDs are separated by PDMS layers, the concentration of each layer can be optimized without assembling dots. This ultimately multiplies the down-converted photons. QDs are absorptive in the UV or near-UV range, and down-convert these high-energy photons into visible photons, which are more effective for photo-current generation in bulk semiconductors. This method enhances the power conversion efficiency of a solar cell by nearly 22% compared to that without CdS QDs. External quantum efficiency (EQE) measurements revealed that dual layers of QDs easily surpass the single and non QD cases, and demonstrate an improvement as high as 1.5 times in the UV region. This study shows the possibility of using PDMS as a medium to increase the amount of QDs without self-assembly and should be considered for the design of next-generation solar cells.

2. Process and structure

Fig. 1 shows the schematic plot of a GaAs solar cell with dual-layer CdS QDs. First, a Si-doped n-type GaAs substrate (1 0 0) substrate was prepared for the deposition of a GaAs single-junction solar cell structure using metal-organic chemical vapor deposition (MOCVD). Silane (SiH_4), and diethylzinc (DEZn) were used as the n-type and p-type dopant sources, respectively. Trimethyl (TM-) sources of aluminum, gallium, and indium were used for group-III precursors. Arsine and phosphine were used as the group V reaction agents. The V/III ratio was kept at approximately 200 at a growth temperature ranging from 600 to 720 °C. The growth rate for all arsine-based layers was kept at 2.0 m/h, and the indium source was precisely controlled by an Epison controller system. The uniformity of bulk layer thickness during epitaxial growth was controlled to less than 0.4% standard deviation in a 3-in wafer. The epitaxial growth started from depositing a 300 nm-thick n+ −GaAs buffer layer, followed by a 100 nm-thick n+ $-Al_{0.3}Ga_{0.7}As$ back-surface-field layer, and a 3.5 μm-thick n-GaAs base layer. A 500 nm-thick p+ −GaAs layer was grown as the emitter layer, and was capped with a p+ $-Al_{0.8}Ga_{0.2}As$ window layer. Finally, the solar cell structures were completed by capping a 300 nm-thick p+ −GaAs contact layer to form an ohmic contact with the electrode. Standard processes, including photolithography, chemical etching, and metallization, were used to fabricate the solar cell devices. The back-side n-contact in the proposed design was formed by evaporating AuGe (250 Å)/Au (5000 Å), whereas the front p-contact consisted of evaporated Ti (250 Å)/Pt (250 Å)/Au (5000 Å). The shadow loss of the front strip contacts was 3.5%, and area of the cells was 1 cm^2. A colloidal CdS QDs with a concentration of 0.5 mg/ml was dispensed directly onto the surface of the GaAs solar cell. A PDMS film was then composed using the spin-coating method. This film was flexible and suitable for use as a separation layer in the subsequent CdS QD deposition. The flexible PDMS was pasted on the first layer CdS of the GaAs solar cell. The CdS QDs was again sprayed onto the surface of the first layer of CdS with a PDMS film using the pulse spray coating (PSC) method to form a second layer of CdS QDs [25]. Pulse spray coating with interval control spray can uniformly disperse CdS QDs on PDMS films. Using a flexible PDMS film to separate the CdS QDs layer, it is possible to control and adjust the effects of photon down-conversion. Thus, the dual-layer CdS of the GaAs solar cell was successfully fabricated. A GaAs without CdS QDs was also fabricated simultaneously as a reference.

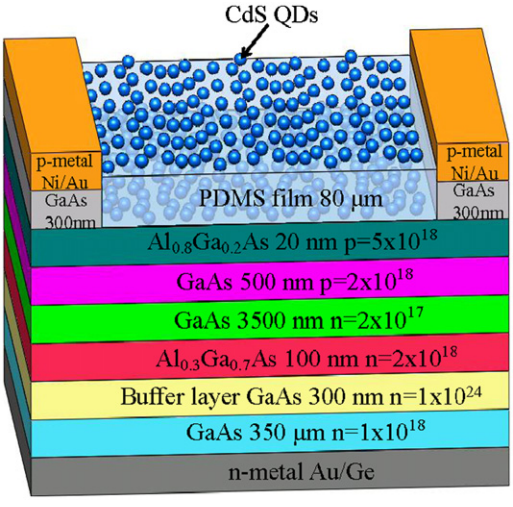

Fig. 1. A schematic plot of the fabricated single-junction GaAs solar cell with dual-layer CdS QDs.

The power conversion efficiencies of GaAs solar cells were measured using a procedure complying with the international standard CEI IEC 60904–1. A 1000 W/m^2, class-A Air Mass 1.5, Global (AM1.5G) light source, consisting of Newport 91192A, Newport 6271A (the Xeon lamp), and an AM1.5G filter (Newport 81088A) was used to characterize the devices [26], and the substrate temperature was kept at 25 ± 1 °C. In addition to the solar simulator, the measurement system also contains a power supply (Newport 69920), a probe stage, and a source meter with a four-wire mode (Keithley 2400). A calibration report by Newport Corporation shows that the temporal instability was 0.88% and non-uniformity was 0.79%. The spectrum of the solar simulator was measured using a calibrated spectrometer (Soma S-2440) at wavelengths ranging from 300 to 1100 nm. Before measurement, the intensity of the solar simulator was calibrated by a monocrystalline silicon reference cell with a 4-cm^2 illumination area (VLSI Standards, Inc.) [27].

For the EQE measurement, we employed a 300 W Xenon lamp (Newport 66984) and a monochromator (Newprot 74112) as the light source. The beam spot at the sample was rectangular, and the spot size was roughly 3 mm^2. Calibration was conducted using a calibrated silicon photodetector with a known spectral response (Newport 818-UV). The EQE measurement was taken using a lock-in amplifier (Standard Research System, SR830), an optical chopper unit (SR540) operating at a 260-Hz chopping frequency, and a 1 Ω resistor in a shunt connection to convert the photocurrent to voltage. The temperature of the cells was actively controlled using the same method in the IV measurement [28,29].

Photoluminescence (PL) and absorption spectra were measured to understand the characteristics of CdS QDs (Fig. 2(a)). The PL emission spectrum of CdS QDs in toluene was measured using

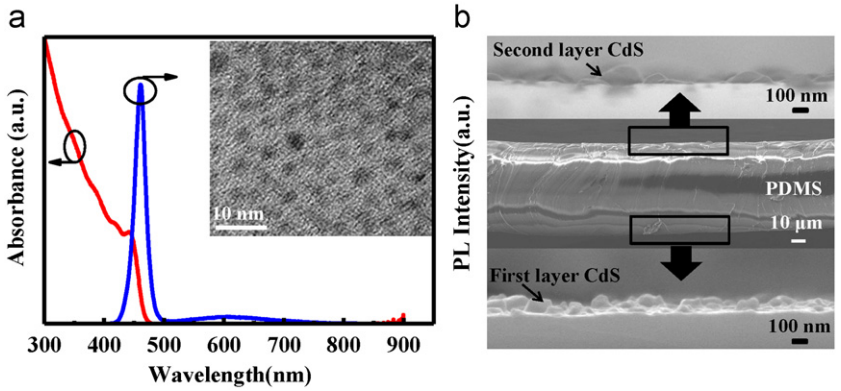

Fig. 2. (a) The measured photoluminescence (blue) and UV–Vis absorbance (red) spectra of CdS QDs in toluene. The peak PL emission wavelength was approximately 460 nm. A TEM image of CdS QDs is shown in the inset. (b) A cross-sectional view of SEM image of PDMS film and dual-layer CdS QDs. (For interpretation of the references to color in this figure legend, the reader is reffered to the web version of this article.)

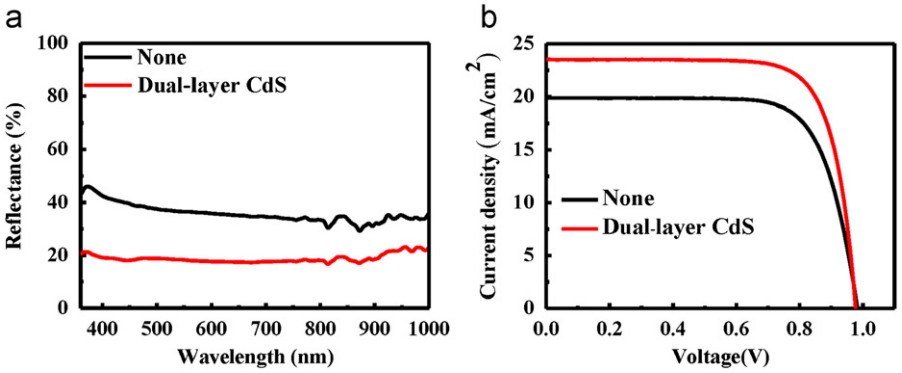

Fig. 3. (a) The reflectance spectra of GaAs solar cell measured with dual-layer CdS QDs (red line) and without CdS QDs (black line). (b) Photovoltaic *I–V* characteristics displaying the superior power conversion efficiency of a GaAs solar cell with dual-layer CdS (red line) compared to one without CdS solar cell (black line) under air mass 1.5 global illuminations and room temperature. (For interpretation of the references to color in this figure legend, the reader is reffered to the web version of this article.)

a 365-nm excited wavelength, and showed two minor peaks at 460 and 600 nm. The absorbance spectrum shows an upward trend from 400 nm and beyond. The CdS QDs can absorb photons in the UV region and then re-emit the visible photons (in this case, they are blue). The inset in Fig. 2(a) shows a transmission electron microscopy (TEM) image of the CdS QDs. Each CdS QD has a diameter of approximately 5 nm, and exhibits a uniform density distribution. Fig. 2(b) shows the cross-section scanning electron microscopic (SEM) image of dual-layer CdS QDs and the flexible PDMS film. The first layer of CdS QDs was distributed directly onto the surface of the window layer in the GaAs solar cell structure. The PDMS film, measuring approximately 80 μm in thickness, was then sprayed and used as the substrate for the second CdS QD layer. The PDMS layer can act as an ARC and prevent further self-assembly when a higher dosage of QDs is desired.

3. Measurement and analysis

Fig. 3(a) shows the measured reflectance spectra of GaAs solar cells with and without dual-layer CdS QDs taken by an integrating sphere with a normal incidence of light. The use of dual-layer CdS QDs in a GaAs solar cell can offer a superior anti-reflective property at wavelengths ranging from 360 to 1000 nm, compared with a cell without CdS QDs. The reduction of reflectance means that more photons can enter the devices; hence, more carriers can be generated, and photocurrent can be increased accordingly. Depositing a CdS QDs layer and layered PDMS onto the surface of a GaAs solar cell reduces the high contrast refractive index between air and the GaAs solar cell because of a composite refractive index gradient [30]. Fig. 3(b) shows the photovoltaic current density–voltage (*I–V*) characteristics of a GaAs solar cell with and without dual-layer CdS QDs. Table 1 lists the measured results of the device parameters. The comparison in this table highlights that dual-layer CdS QD solar cells can effectively enhance the short-circuit current density from 19.87 to 23.52 mA/cm^2 and increase power conversion efficiency from 14.36% to 17.45%. This corresponds to a 22% enhancement, compared to a solar cell without CdS QDs. The open-circuit voltage (V_{oc}) exhibits a negligible change. However, the fill-factor (FF) in a GaAs solar cell with dual-layer CdS QDs also improved, and the serial resistances decreased to 3.84 Ω (compared to 7.93 Ω originally). The major reason for this reduction of electrical resistance is attributed to an increase in the surface photoconductivity cause by the introduction of CdS QDs [31]. To further optimize the dosage of QDs, different weights of the second layer of CdS QDs on the GaAs solar cell were fabricated using the PSC method. The results of the short-circuit current density, open-circuit voltage, FF, and power conversion appear in Fig. 4(a)–(d), respectively. When the amount of CdS QDs increased

Table 1
Current-Voltage Characteristics of GaAs solar cells with and without CdS QDs.

Type	V_{oc} (*V*)	J_{sc} (mA/cm^2)	Fill factor (%)	Efficiency (%)
Dual-layer CdS QDs	0.97	23.52	76	17.45
None	0.97	19.87	74	14.36

to 1.5 mg/cm^2 in the second layer, the maximum power conversion efficiency reached 17.4%. However, other amounts of CdS QDs produced inferior power conversion efficiencies. This may have been caused by the self-assembly of QDs and the resulting reduction of quantum efficiency.

This study uses the spectral response of EQE measurements to further analyze the photon down-conversion and antireflection capability of CdS QDs in a GaAs solar cell. Fig. 5(a) shows the EQE results of GaAs solar cells without and with single-layer and dual-layer CdS QDs. The combination of CdS QDs and a GaAs solar cell exhibits an overall EQE enhancement at a wavelength range of 350–1000 nm. Because the CdS QDs can effectively absorb UV light on the GaAs solar cell surface, the enhanced behavior of the spectral response below 460 nm can be attributed to the photon down-conversion capability. From the EQE measurement, a 1.5-fold enhancement appears between CdS QDs with the PDMS sample and a bare GaAs solar cell. In addition, dual-layer QDs can achieve another 6% increase in EQE when compared to a single layer of QDs. More layers of PDMS are possible for processing, but extra absorption of PDMS must be considered. To estimate the amounts of enhanced performance effectuated by the QD layers, the following expression can calculate the contribution of GaAs solar cells with single-layer and dual-layer CdS QDs in down-conversion [24].

$$J_{sc} = \frac{e}{hc}\int \lambda \times EQE(\lambda) \times I_{AM1.5G}(\lambda)d\lambda \quad (1)$$

where J_{sc} is the short-circuit current density, λ is the photon wavelength, and $I_{AM1.5G}$ is the intensity of the AM1.5G solar spectrum. We can further calculate the percentage that comes from *QD* down-conversion. Ideally, photons shorter than 450 nm are counted as down-converted photons. Eq. (1) shows approximately 10.6% and 12.8% of J_{sc} enhancement coming from this down-conversion in GaAs solar cells with single-layer and dual-layer CdS QDs, respectively. Most of the UV-generated electron–hole pairs in solar cells are near the cell surface. These carriers vanish immediately because of recombination with surface defects, and do not contribute to the final collected current. Hence, with the addition of dual-layer CdS QDs onto the surface

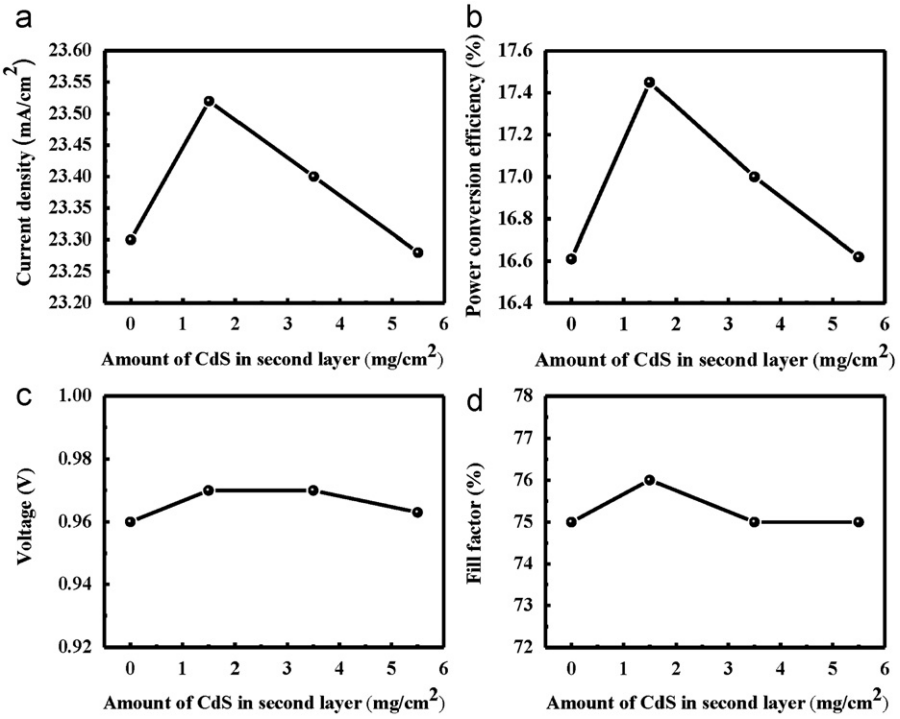

Fig. 4. Evolution of (a) short-circuit current density, (b) power conversion efficiency, (c) open circuit voltage, and (d) fill factor as a function of the increasing amount of CdS QD in the second layer.

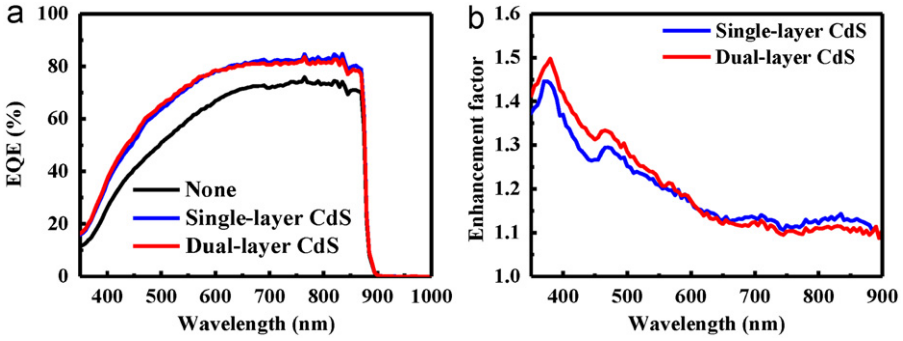

Fig. 5. (a) Measurements of the EQE in the GaAs solar cell without CdS (black line) and with single-layer (blue line) and dual-layer CdS QDs (red line). (b) EQE enhancement factor of GaAs solar cell with single-layer (blue line) and dual-layer CdS QDs (red line). (For interpretation of the references to color in this figure legend, the reader is reffered to the web version of this article.)

of the GaAs solar cell, the CdS QDs emit photons with a visible wavelength. These photons can be absorbed deeper into the bulk region, consequently improving the power conversion efficiency. The photon down-conversion capability can be controlled and adjusted effectively through the number of PDMS layers and the dosage of CdS QDs in each layer. Conversely, this layer acts similarly to an ARC layer in the longer wavelength range, allowing more photons into the solar cell. In this case, a wider range of photon energy can be absorbed, ultimately increasing conversion efficiency.

4. Conclusion

This study investigates the enhanced power conversion efficiency of a GaAs solar cell with dual-layer CdS QDs in a flexible PDMS film. The dual-layer CdS QDs offered more photon down-conversion capability after increasing the CdS QD concentration embedded in a flexible PDMS film. Compared to a GaAs solar cell without CdS QDs, this design achieved an increase of 22% in power conversion efficiency. This increase can be attributed to the photon down-conversion and antireflection mechanism. We suggest that these dual-layer CdS QDs in flexible PDMS film could provide an efficient improvement in GaAs solar cells and other related photovoltaic applications in the future.

Acknowledgments

This study was supported by the National Science Council of Taiwan under grant numbers NSC 99–2120-M-006-002 and NSC-99–2120-M-009-007. C. C. Lin would also like to thank NSC project number NSC101-3113-E-110-006 for financial support.

References

[1] R.R. King, D.C. Law, K.M. Edmondson, C.M. Fetzer, G.S. Kinsey, H. Yoon, R.A. Sherif, N.H. Karam, 40% efficient metamorphic GaInP/GaInAs/Ge multijunction solar cells, Applied Physics Letters 90 (2007) 183516.
[2] M.A. Green, K. Emery, Y. Hishikawa, W. Warta, E.D. Dunlop, Progress in Photovoltaics: Solar cell Efficiency Tables (Version 39), Wiley, 2011.
[3] W. Shockley, H.J. Queisser, Detailed balance limit of efficiency of p–n junction solar cells, Journal of Applied Physics 32 (1961) 510–519.
[4] W.H. Southwell, Gradient-index antireflection coatings, Optics Letters 8 (1983) 584–586.
[5] D. Bouhafs, A. Moussi, A. Chikouche, J.M. Ruiz, Design and simulation of antireflection coating systems for optoelectronic devices: application to silicon solar cells, Solar Energy Materials and Solar Cells 52 (1998) 79–93.
[6] D.J. Aiken, High performance anti-reflection coatings for broadband multi-junction solar cells, Solar Energy Materials and Solar Cells 64 (2000) 393–404.
[7] N. Shibata, Plasma-chemical vapor-deposited silicon oxide/silicon oxynitride double-layer antireflective coating for solar cells, Japanese Journal of Applied Physics 30 (1991) 997–1001.
[8] J.H. Zhao, A.H. Wang, P.P. Altermatt, S.R. Wenham, M.A. Green, 24% efficient PERL silicon solar cell: recent improvements in high efficiency silicon cell research, Solar Energy Materials and Solar Cells 41 (1996) 87–99.
[9] Y. Inomata, K. Fukui, K. Shirasawa, Surface texturing of large area multi-crystalline silicon solar cells using reactive ion etching method, Solar Energy Materials and Solar Cells 48 (1997) 237–242.
[10] Y.A. Chang, Z.Y. Li, H.C. Kuo, T.C. Lu, S.F. Yang, L.W. Lai, L.H. Lai, S.C. Wang, Efficiency improvement of single-junction InGaP solar cells fabricated by a novel micro-hole array surface texture process, Semiconductor Science and Technology 24 (2009).
[11] M.A. Tsai, P.C. Tseng, H.C. Chen, H.C. Kuo, P.C. Yu, Enhanced conversion efficiency of a crystalline silicon solar cell with frustum nanorod arrays, Optics Express 19 (2011) A28–A34.
[12] P.C. Tseng, P.C. Yu, H.C. Chen, Y.L. Tsai, H.W. Han, M.A. Tsai, C.H. Chang, H.C. Kuo, Angle-resolved characteristics of silicon photovoltaics with passivated conical-frustum nanostructures, Solar Energy Materials and Solar Cells 95 (2011) 2610–2615.
[13] K.Q. Peng, X. Wang, X.L. Wu, S.T. Lee, Platinum nanoparticle decorated silicon nanowires for efficient solar energy conversion, Nano Letters 9 (2009) 3704–3709.
[14] T. Stelzner, M. Pietsch, G. Andra, F. Falk, E. Ose, S. Christiansen, Silicon nanowire-based solar cells, Nanotechnology 19 (2008) 295203.
[15] G.R. Lin, Y.C. Chang, E.S. Liu, H.C. Kuo, H.S. Lin, Low refractive index Si nanopillars on Si substrate, Applied Physics Letters 90 (2007) 181923.
[16] Q. Sun, Y.A. Wang, L.S. Li, D.Y. Wang, T. Zhu, J. Xu, C.H. Yang, Y.F. Li, Bright, multicoloured light-emitting diodes based on quantum dots, Nature Photonics 1 (2007) 717–722.
[17] S. Coe, W.K. Woo, M. Bawendi, V. Bulovic, Electroluminescence from single monolayers of nanocrystals in molecular organic devices, Nature 420 (2002) 800–803.
[18] Y.J. Lee, C.J. Lee, C.M. Cheng, Enhancing the conversion efficiency of red emission by spin-coating CdSe quantum dots on the green nanorod light-emitting diode, Optics Express 18 (2010) A554–A561.
[19] L.D. Huang, C.C. Tu, L.Y. Lin, Colloidal quantum dot photodetectors enhanced by self-assembled plasmonic nanoparticles, Applied Physics Letters 98 (2011) 113110.
[20] D.F. Qi, M. Fischbein, M. Drndic, S. Selmic, Efficient polymer-nanocrystal quantum-dot photodetectors, Applied Physics Letters 86 (2005) 093103.
[21] E. Mutlugun, I.M. Soganci, H.V. Demir, Photovoltaic nanocrystal scintillators hybridized on Si solar cells for enhanced conversion efficiency in UV, Optics Express 16 (2008) 3537–3545.
[22] X.D. Pi, Q. Li, D.S. Li, D.R Yang, Spin-coating silicon-quantum-dot ink to improve solar cell efficiency, Solar Energy Materials and Solar Cells 95 (2011) 2941–2945.
[23] C.Y. Huang, D.Y. Wang, C.H. Wang, Y.T. Chen, Y.T. Wang, Y.T. Jiang, Y.J. Yang, C.C. Chen, Y.F. Chen, Efficient Light Harvesting by Photon Downconversion and Light Trapping in Hybrid ZnS Nanoparticles/Si Nanotips Solar Cells, Acs Nano 4 (2010) 5849–5854.
[24] H.C. Chen, C.C. Lin, H.W. Han, Y.L. Tsai, C.H. Chang, H.W. Wang, M.A. Tsai, H.C. Kuo, P.C. Yu, Enhanced efficiency for c-Si solar cell with nanopillar array via quantum dots layers, Optics Express 19 (2011) A1141–A1147.
[25] H.C. Kuo, C.W. Hung, H.C. Chen, K.J. Chen, C.H. Wang, C.W. Sher, C.C. Yeh, C.C. Lin, C.H. Chen, Y.J. Cheng, Patterned structure of remote phosphor for phosphor-converted white LEDs, Optics Express 19 (2011) A930–A936.
[26] ASTMG173-03, Standard Tables for Reference Solar Spectral Irradiances, ASTM International, West Conshohocken, Pennsylvania, 2005.
[27] K.A. Emery, C.R. Osterwald, Solar cell calibration methods, Solar Cells 27 (1989) 445–453.
[28] G.P. Smestad, F.C. Krebs, C.M. Lampet, C.G. Granqvist, K.L. Chopra, X. Mathew, H. Takakura, Reporting solar cell efficiencies in solar energy materials and solar cells, Solar Energy Materials and Solar Cells 92 (2008) 371–373.
[29] P.C. Tseng, P. Yu, H.C. Chen, Y.L. Tsai, H.W. Han, M.A. Tsai, C.H. Chang, H.C. Kuo, Angle-resolved characteristics of silicon photovoltaics with passivated conical-frustum nanostructures, Solar Energy Materials and Solar Cells 95 (2011) 2610–2615.
[30] S.F. Rowlands, J. Livingstone, C.P. Lund, Optical modelling of thin film solar cells with textured interfaces using the effective medium approximation, Solar Energy 76 (2004) 301–307.
[31] C.C. Lin, H.C. Chen, Y.L. Tsai, H.V. Han, H.S. Shih, Y.A. Chang, H.C. Kuo, P.C. Yu, Highly efficient CdS-quantum-dot-sensitized GaAs solar cells, Optics Express 20 (2012) A319–A326.